Spatial variability of hydraulic conductivity and solute transport parameters and their spatial correlations to soil properties

Vanessa A. Godoy[1,2*], Lázaro Valentin Zuquette[1] and J. Jaime Gómez-Hernández[2]

[1] Geotechnical Engineering Department, São Carlos School of Engineering, University of São Paulo. Avenida Trabalhador São Carlense, 400, 16564-002, São Carlos, São Paulo, Brazil.

[2] Institute for Water and Environmental Engineering, Universitat Politècnica de València, Camí de Vera, s/n, 46022, València, Spain

* corresponding author: valmeida@usp.br (+55)16 35739501

Highlights

- We study reactive and non-reactive solute transport in a tropical soil.
- Solute transport parameters and hydraulic conductivity display high variability.
- Solute transport parameters and soil properties present spatial dependence.
- Spatial correlation is important up to 2.5 m.

Abstract

Spatial variation of the correlation among variables related to water flow and solute transport are important in the characterization of the spatial variability when performing uncertainty analysis and making uncertainty-qualified solute transport predictions. However, the spatial variation of the correlation between solute transport parameters and soil properties are rarely studied. In this study, the spatial correlation among laboratory-measured transport parameters dispersivity and coefficient of distribution of a reactive and a nonreactive solute and soil properties were studied at the scale of a few

meters using a dense sampling design. In an area of 84 m^2 and a depth of 2 meters, 55 undisturbed soil samples were taken to determine the soil properties. Column experiments were performed, and the transport parameters were obtained by fitting the experimental data to the analytical solution of the advection-dispersion equation using the computer program CFITM. Stepwise multiple linear regression (MLR) was performed in order to identify the statistically significant variables. The spatial correlation of the variables and between variables were determined using the Stanford Geostatistical Modeling Software. Soil properties presented a moderate coefficient of variation, while hydraulic conductivity and transport parameters were widely dispersed. The difference between its minimum and maximum value was quite large for most of the studied variables evidencing their high variability. Both dispersivity and retardation factor were higher than the expected and this result can be related to the preferential pathways and to the non-connected micropores. None of the physical soil property was strongly correlated to the transport parameters. Coefficient of distribution was strongly correlated to the cation exchange capacity and significantly correlated to mesoporosity and microporosity. Hydraulic conductivity presented significant positive correlation to the effective porosity and macroporosity. Stepwise multiple linear regression analysis indicated that further studies should be performed aiming to include other variables relevant for lateritic soils such as pH, electrical conductivity, the content of Al and Fe, $CaCO_3$ and soil structure and microstructure. The study of the spatial correlation among transport parameters and soil properties showed that the codispersion among the variables is not constant in space and can be important in dictate the behavior of the combined variables. Our results also showed that some variables that were identified as

explanatory in the MLR were not significant in the spatial analysis of the correlation, showing the importance of this kind of analyses for a better decision about the most relevant variables and their relations. The present study was a first attempt to evaluate the spatial variation in the correlation coefficient of transport parameters of a reactive and a nonreactive solute, indicating the more relevant variables and the ones that should be included in future studies.

Keywords: cross-variogram, dispersivity, retardation factor, column experiment, undisturbed soil sample

1. Introduction

The soil's ability to retard and filter solutes as well as water flow and solute movement in soils are significant themes in the earth and environmental sciences, and they are critical in the hydrological and biogeochemical cycles (Keesstra et al., 2012; Kung et al., 2005). Solutes can migrate from the soil to the groundwater and cause its contamination (Arias-Estévez et al., 2008). That ability can be quantified after determining soil transport parameters such as dispersivity (α) and partition coefficient (K_d) (Dyck et al., 2005; Fetter, 1999). Knowledge of solute transport parameters is needed to improve the prediction of the groundwater contamination potential (Kazemi et al., 2008). These parameters depend on many factors such as the chemical characteristics of the contaminant and the soil physical, chemical, and physicochemical properties (Holland, 2004; Trangmar et al., 1986).

The transport parameters, the hydraulic conductivity, other soil properties and the relations among them are highly spatially variable following a structural pattern overlapped by an erratic component, also referred to as structured variation (Alletto and Coquet, 2009; Fu and Gómez-Hernández, 2009; Goovaerts, 1997; Isaaks and Srivastava, 1989; Mulla and Mc Bratney, 2002; Trangmar et al., 1986). The spatial variability of soil properties might be studied at the centimeter scale, as well as at a regional scale since the soil heterogeneity is present in all scales (Chapuis et al., 2005; DeGroot and Baecher, 1993; Lacasse and Nadim, 1996; Søvik and Aagaard, 2003). Additionally, since taking measurements of the properties of interest in an entire area is impractical, there is always an uncertainty component related to the locations where the properties were not measured (Erşahin et al., 2017; Fu and Gómez-Hernández, 2009).

79 The interest in quantifying the uncertainty in groundwater flow and solute transport
80 predictions has increased in the last decades (Cassiraga et al., 2005; Fu and Gómez-
81 Hernández, 2009; Goovaerts, 2001; Grunwald et al., 2004; Hoffmann et al., 2014;
82 Lacasse and Nadim, 1996; Li et al., 2011; Teixeira et al., 2012). Performing an
83 uncertainty analysis and making uncertainty-qualified solute transport predictions
84 requires building a model of the spatial variability of the parameters controlling transport
85 from a limited set of experimental data (laboratory or field). Such a model will allow
86 estimating soil properties at unsampled locations (Goovaerts, 1999).
87 The study of the spatial variability in soil science is commonly performed using
88 geostatistics (Alletto and Coquet, 2009; Erşahin et al., 2017; Goovaerts, 1999; Gwenzi
89 et al., 2011; Marín-Castro et al., 2016). This technique is based on the random function
90 model assumption, where variables are modeled as random variables usually spatially
91 correlated. By assuming this model, the characterization of the spatial variability is
92 reduced to the characterization of the correlations among the random variables of the
93 random function (Goovaerts, 1997). Then, it is possible to perform coherent inferences
94 about the variable using estimation (such as kriging and cokriging) or simulation
95 techniques (such as sequential Gaussian simulation), and the spatial variability can be
96 fully characterized.
97 Geostatistics has been widely used to study the spatial variability of several soil
98 properties (Alletto and Coquet, 2009; Brocca et al., 2007; Goovaerts, 1998; Grego et al.,
99 2006; Iqbal et al., 2005; Mbagwu, 1995; Tesfahunegn et al., 2011; Vieira, 1997; Wang
100 and Shao, 2013; Zhao et al., 2011) and specifically of the hydraulic conductivity (Bohling
101 et al., 2012; Gwenzi et al., 2011; Hu et al., 2008; Liu et al., 2017; Marín-Castro et al.,

2016; Motaghian and Mohammadi, 2011; Sobieraj et al., 2002; Sudicky et al., 2010). On the other hand, the spatial characterization of solute transport parameters is still discrete (Huysmans and Dassargues, 2006; Jacques et al., 1999; Kazemi et al., 2008) due to the high cost and time-consuming efforts associated with solute transport studies (Erşahin et al., 2017) .

Allen-King et al. (2006) determined the spatial geostatistical properties of the perchloroethene partition coefficient (K_d) and permeability (k) and found that K_d and k exhibited a statistically significant positive correlation. They concluded that additional studies were necessary since the statistics describing the horizontal autocorrelation behavior of $ln\ K_d$ and its cross-correlation to $ln\ k$ remained uncertain.

Gómez-Hernández, Fu, and Fernandez-Garcia (2006) studied the impact of the cross-correlation between $ln\ K_d$ and $ln\ K$ in the upscaling of the retardation factor (R) in a synthetic two-dimensional isotropic aquifer. They found that the upscaled R was highly affected by the cross-correlation between $ln\ K$ and $ln\ K_d$. For a negative correlation, upscaled R for early times was smaller than that for late times. For a positive correlation, the result was the opposite and upscaled R for early times was larger than that for late times.

Erşahin et al. (2017) characterized the spatial variability of pore-water velocity (v), dispersivity, retardation factor and dispersion coefficient (D) and analyzed their statistical relations to other soil properties. They found that solute parameters were not correlated with the physical soil properties but were significantly correlated with soil chemical variables such as pH, electrical conductivity (EC) and cation exchange capacity (CEC).

A pure nugget model was fitted to logα and R indicating no spatial structure. On the contrary, *log v* and *log D* showed a moderate and strong spatial structure, respectively.

By analyzing many studies related to spatial variability in soil science, it can be noticed that a multivariate approach is used, in line with Goovaerts (1999), who points out that the soil information is generally multivariate. Usually, multivariate data are analyzed with statistical methods, such as principal component analysis or multiple linear regression (Ferreira da Silva et al., 2013; Rodríguez Martín et al., 2007) but without accounting for their possible spatial correlation (Erşahin et al., 2017; Kazemi et al., 2008). Ignoring the multivariate spatial correlations can be a waste of available and important information.

Some effort has been made to characterize the spatial variation of the correlation among variables and to use this information for estimation purposes (Benamghar and Gómez-Hernández, 2014; Bevington et al., 2016; Goovaerts, 1998; Guagliardi et al., 2013). Nevertheless, attempts to obtain the spatial variation of the correlation among solute transport and all statistically significant variables are rare (Jacques et al., 1999) and more studies need to be done.

Our first objective is to determine the linear statistical correlations among soils properties, K, α, and K_d for a reactive (potassium) and a nonreactive (chloride) solute. Second, in order to identify the more statistically significant variables that explain the variability of the variables of interest (K, α, and K_d), multiple linear regression is performed. The third objective is to model the spatial structures of soils properties and of the variables of interest. Aiming to study the spatial cross-correlation among variables, the fourth objective is to model the relations among the variables of interest and each one of the more statistically significant variables. To the best of our knowledge, this is

147 the first time that the spatial correlations among α and K_d, of a reactive and a
148 nonreactive solute, and statistically significant variables are studied. Finally, although the
149 characterization of the spatial variability of soil properties at the centimeter/meter scale
150 can affect the solute transport prediction at a bigger scale (Salamon et al., 2007),
151 studies in this scale are scarce. In this context, we are interested in the small-scale
152 variability using a dense sampling design.

153 ## 2. Material and methods

154 ### 2.1. Description of the study site

155 The study was carried out in São Carlos city (21°51′38″ S, 47°54′14″ W), which is
156 located in the East-Center of the São Paulo State, Brazil (Fig.1). As mentioned before,
157 since we are studying the spatial variability at the scale of a few meters, the study site
158 covers an area of 84 m^2 and a depth of 2 meters. The pedologic soil type is classified as
159 Oxisol according to US Soil Taxonomy (Soil Survey Staff, 1999) and medium textured,
160 dystrophic, red–yellow Latosol according to the Brazilian classification system (Santos et
161 al., 2014). Clayey fine sand is the predominant texture. The climate in this region
162 is Köppen's Cwa type (Miranda et al., 2015; Peel et al., 2007). The mean annual
163 temperature is 21.2 °C, having humid and hot summers and a dry winter, with an
164 average annual rainfall of 1423 mm (Miranda et al., 2015). The parent material
165 comprising Cenozoic sediments that cover the Botucatu Formation (Paraná Sedimentary
166 Basin, São Bento Group), constituted by unconsolidated sands with the thickness
167 ranging from 5 to 7 m and pebbles at the base, and are spread at all São Paulo interior
168 region (Azevedo et al., 1981; Giacheti et al., 1993). The action of weathering under

tropical conditions makes the soil from the Cenozoic sediments highly lateritized (Giacheti et al., 1993). The main constituents of the studied soil are quartz, oxides, and hydroxides of aluminum, kaolinite, and gibbsite. Macropores and dual-porosity are also characteristics of that soil (Rohm, 1992).

Fig. 1

2.2. Soil sampling

Undisturbed soil samples were cautiously taken from hand-excavated trenches by carefully forcing rigid polyvinyl chloride (PVC) cylinders (150 mm in height and 97.2 mm in inner diameter) into the soil. Soil core sampling started by removing the grass (when present) and a thin and hard layer from the top of the soil. Sampling in the x-y plane was performed at 23 locations of the study site. For each x-y coordinate three samples were taken at different depths (z coordinate 0.5 m, 1.0 m and 1.5 m), resulting in a dense sampling design. Initially, 69 undisturbed soil samples were collected, but 14 samples presented defects or cracks and were discarded. The position of the 55 remaining samples in the study site is shown in Fig.1. Additionally, disturbed soil samples were collected to characterize soil properties that were not spatially evaluated.

2.3. Soil properties characterization

Silt, clay and sand content, cation exchange capacity (*CEC*), total porosity (*n*), effective porosity (*ne*), macroporosity (*Ma*), mesoporosity (*Me*), microporosity (*Mi*) and bulk density (ρ_d) are referred to soil properties. These soil properties were analyzed spatially. In the laboratory, the moisture was determined in three replicates for each soil sample.

191 Subsequently, the soil was air-dried and sieved through a #10 mesh sieve (2 mm
192 openings). Particle size distribution were determined according to ASTM D7928-17
193 (ASTM, 2017a) and ASTM D6913 / D6913M-17 (ASTM, 2017b). in only one replicate for
194 each soil sample. Particle density ρ_s was determined in five replicates using the ASTM D
195 854-14 (ASTM, 2014a) and resulted in 2.71 $Mg \cdot m^{-3}$ for all soil samples (arithmetic mean
196 of all replicates).
197 Bulk density was determined for each soil column as $\rho_d = M_d/V_t$, where V_t is the total
198 volume of the soil sample (internal volume of each PVC cylinder) and M_d is the dry mass
199 of the soil sample.
200 Mercury intrusion porosimetry (MIP) (Washburn, 1921) and total porosity was calculated
201 for each soil sample as $n = 1 - \rho_d/\rho_s$. When the total porosity calculated was different
202 from the one obtained by MIP, we assumed that the difference was due to large pores
203 that were not identified in the MIP due to the reduced sample size used. The effective
204 porosity (*ne*) was considered as the total porosity minus the porosity that corresponds to
205 the soil water content at 33 kPa, suction equivalent to the field capacity (Ahuja et al.,
206 1984; Brutsaert, 1967; Corey, 1977; Dippenaar, 2014). It is important to mention that the
207 field capacity is not precisely defined in soil science and we chose to use that value
208 since it is widely used in the literature. The diameter of the pore equivalent to the suction
209 at 33 kPa was calculated as 8.9 μm from the capillary rise equation assuming a contact
210 angle of 0º. Thus, based on the results of the MIP, the effective porosity was calculated
211 as the total porosity minus the porosity correspondent to the pores with a diameter
212 smaller than 8.9 μm. From the MIP results, *Ma*, *Me*, and *Mi* were determined according
213 to the classification proposed by Koorevaar et al. (1983), in which the diameters of *Mi*,

214 *Me*, and *Ma* are, respectively, <30 μm, 30-100 μm and >100 μm. The methylene blue
215 adsorption test using the filter paper method described by Pejon (1992) was used to
216 determine *CEC* in one replicate for each soil sample.
217 In order to characterize average properties with no concern about spatial structure, the
218 next parameters were determined in three replicates by using disturbed soil samples: pH
219 in H_2O and in KCl, redox potential (Eh) and electrical conductivity (*EC*) (Donagema and
220 Campos, 2011), ΔpH ($pH_{KCl} - pH_{H2O}$) (Mekaru and Uehara, 1972), point of zero charge
221 (PZC) ($2pH_{KCl} - pH_{H2O}$) (Keng and Uehara, 1974), organic matter content according to
222 the ASTM D 2974-14 (ASTM, 2014b), and mineralogical composition by X-ray diffraction
223 (Azaroff and Buerger, 1953).

224 **2.4. Column experiments**

225 The PVC cylinders used for collecting the undisturbed soil samples were used as rigid-
226 wall permeameters and 55 column experiments were conducted. Figure 2 shows the
227 column experiments in progress. First, the columns were sealed with a cap containing a
228 stainless plastic plate with holes on both ends of the column, which allowed a uniform
229 distribution of the inlet flow. Second, the soil samples were slowly saturated from the
230 bottom with deionized water to remove entrapped air. Third, the flow was reversed, and
231 the permeability test was performed under a constant hydraulic gradient of 1 and the
232 flow rate (*Q*) was measured. We have taken two measures per day and we assumed
233 that steady-state flow was achieved when *Q* variations were below 5% in a week. Water
234 temperature was monitored throughout the test and, when necessary, corrections were
235 made in the calculations of the hydraulic parameters. Fourth, the following water flow
236 parameters were obtained from each soil sample: saturated hydraulic conductivity, *K*;

specific discharge, q; flow rate, Q; and average linear velocity, v (q/ne) (Freeze and Cherry, 1979). When the steady-state flow was reached, deionized water was replaced by a 2.56 mol m^{-3} KCl solution (100 mg L^{-1} K^+ and 90.7 mg L^{-1} Cl^- referred to as initial concentrations, C_0) continuously injected into the soil column. Solute displacement tests were carried out under constant hydraulic head and isothermal (20 °C) conditions. The concentration, temperature, and pH of the initial solution were monitored throughout the test. Leachate samples were collected from the outlet of the columns at pre-set time intervals (defined for each column in accordance with the flow rate), stored in plastic bottles and refrigerated immediately after collection. Preferably, the tests were performed until the relative concentrations (C/C_0) reached 1, but this condition was not achieved in some samples. An ion-selective electrode (ISE) (Hanna instruments - HI 4107 model) was used to determine Cl^- concentration (C) at each time. K^+ concentration at each time was measured by a flame photometer (Micronal B462 model) at a 1:21 ratio. All ion concentrations were measured in one replicate and determined as the arithmetic mean of the replicates. The relative concentrations (C/C_0) of Cl^- and K^+ were determined by dividing the concentration of the ion in the leachate samples at each time by the concentration of the ion in the initial solution. Thereafter, a breakthrough curve (BTC) of each soil sample and each ion was plotted. The BTC's were expressed as C/C_0 and the number of pore volumes (T), where T is a dimensionless variable calculated as $T = vt/L$ (van Genuchten, 1980), where v is the average linear velocity, t is the time elapsed from the start of the solute application, and L is the length of the soil column (150 mm).

Fig. 2

2.5. Transport parameter determination

Dispersivity (α) [L] and partition coefficient between liquid and solid phases (K_d) [L^3M^{-1}] are referred to as the transport parameters and were determined as explained next.

The advection-dispersion equation (ADE) used to interpret the BTCs is

$$R\frac{\partial C}{\partial t}=D\frac{\partial^2 C}{\partial x^2}-v\frac{\partial C}{\partial x}, \qquad (1)$$

where C is solute concentration [ML-3], D is the hydrodynamic dispersion coefficient [M2T-1], R is the retardation factor [-], x is the distance [L], and t is time [T].

The hydrodynamic dispersion coefficient is related to the dispersivity by

$$D=\alpha \cdot v, \qquad (2)$$

and the retardation factor is related to the partition coefficient Kd through the expression

$$R=1+\frac{\rho_d}{n}K_d, \qquad (3)$$

This equation has the following analytical solution (Lapidus and Amundson, 1952; Ogata and Banks, 1961), when the initial condition is C_0=0 for the entire sample, and the boundary conditions are C=C_0 at the inlet and C=0 at an infinite distance from the inlet

$$\frac{C}{C_0}=\frac{1}{2}\left[\operatorname{erfc}\left(\frac{RL-vt}{2\sqrt{DRt}}\right)\right]+\frac{1}{2}\exp\left(\frac{vL}{D}\right)\operatorname{erfc}\left(\frac{RL+vt}{2\sqrt{DRt}}\right), \qquad (4)$$

where erfc is the complementary error function.

This expression was fitted to the observed BTCs for each soil sample and values of D and R were obtained for both K^+ and Cl^-. The fitting was performed using the computer program CFITM (van Genuchten, 1980), that is part of the Windows-based computer software package Studio of Analytical Models (STANMOD) (Šimůnek, van Genuchten, Šejna, Toride, & Leij, 1999).

2.6. Statistical analysis

Exploratory analysis of the K, *ln K*, soil properties and transport parameters (including *P*, *R*, *D*, *ln α* of K^+ and *ln α* of Cl^-) was performed. Global summary statistics such as mean, standard deviation, variance, minimum and maximum value, kurtosis, skewness, and coefficient of variation (CV) were computed. The CV were classified according to Wilding and Drees (1983): low variability for CV < 15%; moderate variability for 15% < CV < 35%; and high variability for CV > 35%. The normality of the data was tested by means of the Kolmogorov–Smirnov test (Massey, 1951). When necessary, the variables were standardized, and the subsequent studies were performed using standard normal variables. Outliers were analyzed in detail to investigate errors in the determination of the variables, and when deemed appropriate they were excluded from the dataset. Trends were also investigated and, if present, removed. The presence and strength of significantly linear associations between soil properties and the variables of interest (*ln K*, *ln α* (K^+), *ln α* (Cl^-), *Kd* (K^+), and *Kd* (Cl^-)) were examined by computing Pearson correlation coefficients at 0.05 and 0.01 significance level. The natural logarithm (ln) of *α* and *K* were used as variables rather *α* and *K* because they resulted in better correlations.

The quantification of the significance of the relationships between all the studied variables, i.e. soil properties and variables of interest, was analyzed separately using multiple linear regression (MLR) (Eq. 3). Stepwise regression analyses were carried out to avoid the possible collinearity effects in multiple regressions. Statistically significant differences were set with p values equal to 0.05.

A stepwise MLR as in Equation (3)

$$y = b_0 + b_1 w_1 + b_2 w_2 + b_3 w_3 + \ldots + b_n w_n \quad (3)$$

defines the best linear combination of the variables to predict the variables of interest and helps understand which variables have the highest influence on the variables of interest,

where y is the dependent variable and w_1 to w_n are independent variables.

2.7. Geostatistical analysis

Based on the MLR results, the spatial dependence of the more statistically significant soil properties and the variables of interest was measured using direct experimental variograms.

The variogram can be defined as the mean-squared difference between the same variable at specified separation distances (Isaaks and Srivastava, 1989), and it was calculated using

$$\gamma(\mathbf{h}) = \frac{1}{2N} \sum_{aa=1}^{N(\mathbf{h})} [z(u_{aa}) - z(u_{aa} + \mathbf{h})]^2 \quad (5)$$

where $\gamma(\mathbf{h})$ is the variogram function, $z(u_\alpha)$ is the measured value of the attribute under consideration taken at location aa, $\mathbf{h}$ is the separation vector and $N(\mathbf{h})$ is the number of data-pairs separated by the vector $\mathbf{h}$. The variograms were obtained using the Stanford Geostatistical Modeling Software (SGeMS).

Almost all experimental variograms were best fitted to the isotropic spherical variogram model (Isaaks and Srivastava, 1989)

$$\gamma(\mathbf{h}) = c_0 + c_1 sph(|\mathbf{h}|, a) \quad (6)$$

where *a* is the range, i.e., is the separation distance beyond which observations are spatially independent of each other, c_0 is the nugget effect, c_1 is the covariance contribution or sill value, and **h** is the directional lag distance.

The nugget effect model was also used in a situation, indicating that the variable was randomly spatially distributed.

$$\gamma(\mathbf{h}) = \begin{cases} 0 & if\ \mathbf{h} = 0 \\ 1 & otherwise \end{cases} \qquad (7)$$

In multivariate geostatistics, to model the coregionalization between p variables requires modeling p (p+1)/2 direct and cross-variograms. In this paper, p corresponds to the variables of interest plus the set of variables that best explains its variability, according to the MLR results.

The cross-variogram function describes the way in which two variables are spatially related, and was used to quantify the structure of the spatial correlation between selected soil properties and *ln K*, *ln α* (K^+), *ln α* (Cl^-), K_d (K^+), and K_d (Cl^{-1})

$$\gamma_{uv}(\mathbf{h}) = \frac{1}{2N(\mathbf{h})} \sum_{i=1}^{N(\mathbf{h})} [z_i(u_{aa}) - z_i(u_{aa} + \mathbf{h})] \cdot [z_j(u_{aa}) - z_j(u_{aa} + \mathbf{h})] \qquad (8)$$

where $z_i(u_{aa})$ and $z_j(u_{aa})$ are the measured z_i and z_j regionalized variables, respectively, taken at location *aa*.

The codispersion coefficient, r_{uv}, between the variables *v* and *u*, r_{uv}, for each vector **h** was computed for any pair of variables as the ratio of the cross-variogram between *v* and *u* to the square root of the product of the variograms of *u* and *v* (Goovaerts, 1994)

$$r_{uv}(\mathbf{h}) = \frac{\gamma_{uv}(\mathbf{h})}{\sqrt{\gamma_u(\mathbf{h})\gamma_v(\mathbf{h})}} \qquad (9)$$

3. Results and discussion

3.1. Average soil properties

The main minerals present in the studied soil are quartz, kaolinite, and gibbsite, in accordance with Giachetti *et al.* (1993) and Kronberg *et al.* (1979). Average values of 5.71 and 5.19 for pH in H_2O and in KCl, were obtained, respectively. These results show that the soil is strongly acid, which is a typical characteristic of Cenozoic sediments and lateritic soils (Fagundes and Zuquette, 2011; Giacheti et al., 1993). The negative ΔpH (-0.52) and a point of zero charge (PZC) (4.67) lower than the pH_{H2O} indicate a predominance of negative charges, which can promote cation adsorption (Fagundes and Zuquette, 2011). This soil contains a small average amount of organic matter (2.40 %), a result suitable for lateritic acid soils (Mahapatra et al., 1985). According to the soil salinity classification of the Food and Agriculture Organization of the United Nations (FAO), the electrical conductivity values indicate small amounts of dissolved salts (55.70 mS m^{-1}) and a non-saline soil (Abrol et al., 1988).

3.2. Soil properties statistical analysis

The exploratory statistical results of the soil properties, *v* and *K* are shown in Table 1. In order to identify trends, all statistical results were also investigated for each depth (results not shown), and no significant influence of the depth was observed. Because of that, in further analysis the samples were considered as a unique dataset, regardless of the depth. Soil properties are slightly skewed, quantified by a skewness < |0.5| (Webster, 2001), except *Ma* and *CEC*, which are moderately and highly skewed with a skewness of 0.75 and 1.06, respectively. The difference between its minimum and maximum value

was quite large for K, *ln K*, *v*, silt content, *Ma*, and *CEC*. According to the CV classification of Wilding and Drees (1983), high CV were identified for *K*, *v*, silt content and *Ma* (1.22, 1.23, 0.61 and 0.56, respectively) evidencing high variability in these variables. Our results confirm that soil heterogeneity is present even on a small scale, depending on the studied property (Chapuis et al., 2005; Lacasse & Nadim, 1996; Søvik & Aagaard, 2003).

Mercury intrusion porosimetry results indicated that the soil has dual-porosity and the predominant pore diameters correspond to *Me* and *Mi*. The multimodal pore size distribution is characteristic of well-structured soils (Hajnos, Lipiec, Świeboda, Sokołowska, & Witkowska-Walczak, 2006; Lipiec et al., 2007). The soil has a low *CEC* (maximum value 4.20 cmolc Kg^{-1}) and it suggests a low capacity to adsorb cations by electrostatic adsorption (Fagundes & Zuquette, 2011). Mean soil properties presented values in accordance with the typical characteristics of the studied soil (Giacheti et al., 1993; Zuquette & Palma, 2006), and are shown in Table1.

Table 1

3.3. Statistical analysis of the transport parameters

The breakthrough curves (not shown) of K^+ and Cl^- obtained from the 55 miscible displacement tests were analyzed, and transport parameters were determined. The goodness of fit of the experimental BTC to the ADE model was evaluated by its R^2. Most BTCs presented significant tailing, R^2 ranged from 0.77 to 0.99 with a mean of 0.92 for K^+ and 0.95 for Cl^-, suggesting that the ADE model was suitable to describe the data.

389 BTCs that presented low R^2 were investigated to check for problems in the soil samples,
390 but no problems were found.
391 Basic statistics of the transport parameters are shown in Table 2. Almost all transport
392 parameters were high right-skewed. Moderate right-skewness was obtained only for *R*
393 (Cl^-) and K_d (Cl^-). Slightly right-skewness was obtained for *ln α* (K^+) and *ln α* (Cl^-). High
394 right-skewness bromide (Br^-) *α* and *D*, and moderate *ln α* left-skewness was found in the
395 work of Erşahin et al. (2017).

396 All transport parameters show high CVs and the highest ones were obtained for the
397 reactive solute (K^+). The coefficients of variation of *R* and K_d for K^+ shown that transport
398 parameters are very variable. The values we obtained for *α* were high when compared
399 to other studies using samples of approximately the same dimensions (Erşahin et al.,
400 2017). Also, mean *α* values were high when compared to the typical values used in the
401 literature ($\alpha = 0.1L$, where L in the distance) (Freeze & Cherry, 1979). These differences
402 can be attributed to numerous factors such as the scale of the experiment, flow rate, and
403 boundary conditions. Higher values of *α* can also be indicative of preferential flow.
404 The maximum and minimum values were quite different for all transport parameters,
405 evidencing, again, the large variability in these parameters. Peclet numbers ranged from
406 0.11 to 13.41, showing that for some soil samples the advective transport prevailed,
407 whereas for other samples, dispersive transport was the primary mechanism. These
408 differences probably are related to heterogeneities between physical characteristics of
409 soil samples. *R* (K^+) ranged from 0.69 to 36.19, while *R* (Cl^-) ranged from 0.33 to 5.20, as
410 expected because reactive solute should have larger *R* values than nonreactive solutes.

411 Even though clay content was significant, high *R* (K^+) and *R* (Cl^-) values were not
412 expected since the combination of the clay minerals identified, the low *CEC* values and
413 the predominance of negative charges do not favor the retardation of K^+ and Cl^-. We
414 believe that the structure of the soil played an essential role on the retardation.
415 Moreover, the results of *P* and *R* can be explained by the distribution of the diameter of
416 the pores in the soil, since the maximum *Ma* and *Mi* values were 0.15 and 0.36,
417 respectively. Because of that, part of the solutes can move fast because of advection (in
418 macropores) and part of them can be retarded due to the percolation through
419 micropores and non-interconnected pores, behavior also stated by others (Jarvis, 2007;
420 Silva, van Lier, Correa, Miranda, & Oliveira, 2016; van Genuchten & Wierenga, 1976).

421

422 **Table 2**

423 **3.4. Correlation among variables**

424 To examine the relationship among soil properties, hydraulic conductivity and transport
425 parameters, correlation coefficients were computed. Outliers were removed before the
426 coefficients were computed and the analyses were performed using 50 values for each
427 variable. As none of the variables was normally distributed, correlation analyses were
428 performed using the original data (results not shown) as well as the standardized normal
429 distributed transformed values. As the best correlation coefficients were obtained with
430 standardized variables, all analyzes hereafter were performed using these variables.
431 Variables that are not intrinsic properties of the media such as *P*, *D*, *R*, and *v*, were not
432 considered in the analysis of correlations.

433 None of the physical soil property was strongly correlated to the transport parameters.
434 According to Vanderborght and Vereecken (2007), texture has no significant effect in α
435 and this result is also verified in our study. Since the studied soil has a structure
436 characteristic of lateritic soils by forming agglomerates, texture itself may not show much
437 about dispersivity.

438 It was obtained a statistically significant positive correlation between *ln* α (Cl^-) and ρ_d and
439 a negative correlation with *n*. This result is in accordance with the equation that relates
440 dispersivity to *D* and *v* (*D* = αv, where *v* = *q*/*ne*). Since *n* is slightly negatively related to
441 *ne*, as shown in Table 3, when *v* increases α decreases, justifying the relations obtained.
442 The only variable significantly positively correlated to *ln* α (K^+) was *ln* α (Cl^-), suggesting
443 that higher *D* smaller the influence of other soil properties.
444 A strong positive correlation was obtained between K_d (K^+) and *CEC* and K_d (Cl^-),
445 showing the importance of the physico-chemical adsorption and the relation between the
446 ions studied. A low, but still significant, positive correlation among K_d (K^+) and *Me* was
447 obtained. A negative correlation was obtained between K_d (K^+) and *Mi*, indicating that
448 neither *Ma* nor *Mi* contributed to higher *R*, contrary to our initial assumptions. A low
449 positive correlation was presented by K_d (Cl^+) with silt content and a strong positive
450 correlation with *CEC* and K_d (K^+) and no correlation with pore size was observed.
451 Almost no correlation was obtained among *CEC* and clay content, indicating that the
452 clay mineral present in the soil is not relevant to adsorb cations, as mentioned before.
453 Significant positive correlations among *ln K*, *n*, *ne*, and *Ma* were verified, indicating that
454 these properties dictate the values of *ln K* and of the water flow in soils (Biswas & Si,
455 2009). In a previous study, a high positive correlation was obtained among *K*, *Ma*, and *n*

(Mbagwu, 1995). A significant negative correlation was also found among *ln K* and ρ_d, results in accordance with other studies (Bevington et al., 2016; Botros, Harter, Onsoy, Tuli, & Hopmans, 2009; Mbagwu, 1995; Papanicolaou et al., 2015). These results show the higher *ne* (negatively related to n as shown in **Error! Reference source not found.**), higher *v*, as expected. No significant correlation between *ln K* and texture was obtained. However, this result contrast with several previous studies in non-lateritic soils, showing the impact of the soil agglomerates in the relation among soil properties (M. Huang, Zettl, Lee Barbour, & Pratt, 2016; Igwe, 2005; Nemes, Timlin, Pachepsky, & Rawls, 2009; Pachepsky & Rawls, 2004; Søvik & Aagaard, 2003).

Table 3

Table 4 presents the results of the stepwise multiple linear regression analysis at a significance level of 95%. This analysis was used for investigating the significance of the relationships among all selected variables. The best model for K_d (K^+) was obtained by considering two variables, *CEC* and *Ma*, explaining 70% of the total variance in the model, with Pearson coefficient r equal to 0.84. The model that best represents K_d (Cl^-) was found by combining *CEC*, clay content and Me, which explain 60% of the total variability with a moderate *r* equal to 0.70. These results suggest that other variables that were not considered in this study could be added to better explain the total variability of K_d. For example, several authors have suggested that pH, EC, the content of Al and Fe, $CaCO_3$ and organic carbon have a strong influence on the total variability of K_d (Che, Loux, Traina, & Logan, 1992; Erşahin et al., 2017; Porfiri, Montoya,

Koskinen, & Azcarate, 2015). Additionally, some variables that were significantly correlated to K_d in the correlation analysis were not significant in the MLR. This can be related to possible collinearity effects of these variables, what is identified and excluded by using stepwise method.

The only variables that were significant to model *ln α* (K^+) and *ln α* (Cl^-) were *ln α* (Cl^-) and *ln α* (K^+), respectively, and both have explained only 50% of the total variability, with a moderate *r* equal to 0.70 and 0.72, respectively. It demonstrates that other variables should be considered to better explain total variability in *ln α*. As *α* has some scale and spatial dependence (Erşahin et al., 2017; Freeze & Cherry, 1979), it could be interesting to take into account its spatial relationship with other parameters and not only the parameter itself.

Only 40% of the total variability of *ln K* was explained by the combination of *ne*, ρ_d, and *Ma* with a moderate *r* equal to 0.63. Contrary to the correlation analysis, where the correlation between *n* and *ln K* was statistically significant, in the MLR, *n* had not explained *ln K* variability when combined with other variables. In future studies, it would be valuable to include other explanatory variables, such as soil structure and microstructure that in previous studies were recognized as direct drivers of *K* (Benegas, Ilstedt, Roupsard, Jones, & Malmer, 2014; Beven & Germann, 2013; Burke, Mulligan, & Thornes, 1999; Hillel, 2004; Nanzyo, Shoji, & Dahlgren, 1993; Narwal, 2002; Zimmermann & Elsenbeer, 2008) and can be even more important for lateritic soils.

Table 4

3.5. Spatial correlation among variables

As the correlation among variables in Table 3 neglects the spatial component of the sample points, in this section, the direct and the cross-variograms are used to explore further the spatial correlation among variables. The spatial structure of the standardized variables was evaluated using variograms functions. Table 5 summarizes the parameters of the models that were used to fit the experimental variograms. Only clay content shows no spatial dependence (pure nugget effect), indicating that this variable is spatially random, despite being correlated to sand and silt content, which display spatial dependence. This result can be related to the more or less uniform distribution of the clay content in the studied site, with a CV of only 9%. Experimental variograms of all the remaining variables were fitted with a spherical model, indicating that abrupt changes in space may occur, while preserving an overall spatial structure.

The spatial structure was similar for all the studied variables. The largest range was obtained for *ln K* (4.0 m), while silt content and Mi presented the smallest ones (2.5 m). Microporosity, as well as all studied solute transport parameters, displayed a nugget effect behavior, which accounts for short-scale spatial variability or measurement errors. These variables had a moderate spatial dependence classified by measuring the nugget ratio (R_b = nugget/sill*100%), which is strong if R_b < 25%, moderate if 25% < R_b < 75%, weak if R_b >75% (Cambardella et al., 1994). Variograms of K_d resulted in a greater range than *ln α* variograms. Gupte et al. (1996), found a maximum range of 2.3 m for Br^- dispersivity. Contrary Erşahin et al. (2017) reported no clear spatial structure for *α* and R under their sampling scheme. They argued that *α* is distance and time-dependent at both the column and field scale, which complicates its spatial structure. Jacques et

524 al.(1999) found pure nugget effect in the variogram of K_f (Freundlich partition
525 coefficient). Spatial structure of the Cl^- mass recovery was studied in a 2 m x 2 m x 2 m
526 cube and a range of 0.37 m was found. With these results, we can argue that the range
527 of the studied variables may vary depending on the sampling scheme and on the size of
528 the studied site.

529

530 **Table 5**

531

532 Since the correlation among variables may depend on the spatial structure, the variation
533 of the correlation coefficient among variables with the spatial scale was quantified. Fig.3
534 (A to D) shows these results for the correlations between *ln K*, *ln α* (K^+), *ln α* (Cl^-), K_d
535 (K^+), and K_d (Cl^-) and the variables which explained their variability, according to the
536 MLR results. As stated by Wackernagel (1995), if the codispersion among the variables
537 is constant in space, the structure of correlation of the variables is not affected by spatial
538 scale.
539 The correlation coefficient among *ln K* and *Ma* (Fig.3 A) decreases until 2.2 m and from
540 then on presents a variation around zero, showing that for distances larger than 2.2 m
541 these variables are no longer correlated. The spatial correlation among *ln K* and *ne*
542 (Fig.3 A) showed that until 1.1 m the relationship became stronger and negative,
543 changing completely the kind of relation between these variables since it is recognized
544 that the increase in *ne* favors the water flow in soils. After that, the values became more
545 positive (an expected relation) but the correlation weaker until 2.8 m, when the variation
546 remained near zero. Similar behavior was also verified for the relation between ρ_d and

547 *Ma* and between *ne* and *Ma* (Fig.3 A), but the correlations were not statistically
548 significant. Contrarily, the correlation coefficient between *ln K* and ρ_d became weaker
549 and positive until 3.3 m and then the variables seem to be not related in space. The
550 relation between *ne* and ρ_d was around zero for all studied distances (Fig.3 A).
551 The spatial correlation between K_d (K^+) and *CEC* (Fig.3 B) presented a fast decrease
552 until 1 m and then these variables are no longer statistically significant. The spatial
553 correlation among K_d (K^+) and *Ma* and among *CEC* and *Ma* (Fig.3 B) was not significant
554 even for the distance equal to zero, but these variables were identified as explanatory in
555 the MLR, illustrating the importance of the spatial analyses for a better decision about
556 the most relevant variables and their relations.
557 Until a distance of 1m, only a slight decrease (become more negative) was observed in
558 the spatial correlations among K_d (Cl^-) and *Me*, *Me* and clay content, and *CEC* and *Me*
559 (Fig.3 C). Contrarily, the correlation between K_d (Cl^-) and clay content (Fig.3 C) showed
560 a slight increase until 1m. From 1 m, those correlations increased slightly and ranging
561 near zero, except the correlation between *CEC* and *Me*, which showed an erratic
562 behavior that may be related to its poor spatial correlation. The correlation among K_d (Cl^-
563) and CEC (Fig.3 C) became weaker and negative until 2 m but was statistically
564 significant just until 1.5 m. No spatial correlation was obtained between *CEC* and clay
565 content, result different from that obtained by Jacques et al. (1999) who observed a
566 strong spatial correlation between *CEC* and clay content until 2.03 m. Statistically
567 significant correlation was verified between *ln* α (K^+) and *ln* α(Cl^+) (Fig.2 D) until 1.5 m,
568 and from 2 m these variables were no longer correlated.
569

570 **Fig. 3**

571 ## 4. Conclusions

572 In this study, the spatial correlation among soil properties (total porosity, effective
573 porosity, cation exchange capacity, macroporosity, microporosity, mesoporosity, bulk
574 density, silt, clay and sand content) and the variables of interest (hydraulic conductivity,
575 partition coefficient and dispersivity of a reactive (K^+) and for a nonreactive solute (Cl^-)
576 was studied at the scale of a few meters using a dense sampling design. The soil was
577 characterized as acid with low cation exchange capacity and composed of minerals
578 commons for lateritic soils.

579 None of the variables studied were normally distributed. Soil properties presented a
580 moderate coefficient of variation (CV) while hydraulic conductivity and transport
581 parameters were widely dispersed. None of the physical soil property was strongly
582 correlated to the transport parameters. Nevertheless, some parameters such as cation
583 exchange capacity and partition coefficient presented exhibits a statistically significant
584 positive correlation with transport parameters. Stepwise multiple linear regression (MLR)
585 analysis indicated that further studies should be performed aiming to include other
586 explanatory variables such as pH, electrical conductivity, the content of Al and Fe,
587 $CaCO_3$ and soil structure and microstructure, that are relevant variables for lateritic soils.

588 Our findings show that the use of geostatistical methods was efficient to evaluate the
589 spatial variation in the correlation coefficients. However, for the conditions analyzed, the
590 use of the spatial correlation among transport parameters and soil properties would
591 probably improve the estimation only in a small-scale study, since the spatial correlation

592 were only observed up to 2.5 m. It is important to mention that the study was performed
593 for a specific field site and the results obtained may explain the spatial relation to the
594 studied soil. However, the application of the statistical parameters to estimate transport
595 parameters and predict solute transport in other soil is thus questionable.

596 The present study was a first attempt to evaluate the spatial correlation of transport
597 parameters of a reactive and a nonreactive solute. We showed the soil properties that
598 may exert greater influence and suggested the one that should be included in future
599 studies. Understanding the spatial relations between variables can be useful in perform
600 reliable prediction of flow and solute transport and contribute to reducing uncertainties
601 when studying groundwater contamination.

602

Acknowledgements

The authors thank the financial support by the Brazilian National Council for Scientific and Technological Development (CNPq) (Project 401441/2014-8). The doctoral fellowship awarded to the first author by the Coordination of Improvement of Higher Level Personnel (CAPES) is gratefully acknowledged. The first author also thanks to the international mobility grant awarded by CNPq, through the Science Without Borders program (grant number: 200597/2015-9), and the international mobility grant awarded by Santander Mobility in cooperation with the University of São Paulo.

References

Abrol, I.P., Yadav, J.S.P., Massoud, F.I., Food and Agriculture Organization of the United Nations., Food and Agriculture Organization of the United Nations. Soil Resources Development and Conservation Service., 1988. Salt-affected soils and their management, FAO soils bulletin. 39. Food and Agriculture Organization of the United Nations.

Ahuja, L.R., Naney, J.W., Green, R.E., Nielsen, D.R., 1984. Macroporosity to Characterize Spatial Variability of Hydraulic Conductivity and Effects of Land Management1. Soil Sci. Soc. Am. J. 48, 699. doi:10.2136/sssaj1984.03615995004800040001x

Allen-King, R.M., Divine, D.P., Robin, M.J.L., Alldredge, J.R., Gaylord, D.R., 2006. Spatial distributions of perchloroethylene reactive transport parameters in the Borden Aquifer. Water Resour. Res. 42. doi:10.1029/2005WR003977

Alletto, L., Coquet, Y., 2009. Temporal and spatial variability of soil bulk density and near-saturated hydraulic conductivity under two contrasted tillage management systems. Geoderma 152, 85–94. doi:10.1016/j.geoderma.2009.05.023

Arias-Estévez, M., López-Periago, E., Martínez-Carballo, E., Simal-Gándara, J., Mejuto, J.C., García-Río, L., 2008. The mobility and degradation of pesticides in soils and the pollution of groundwater resources. Agric. Ecosyst. Environ. doi:10.1016/j.agee.2007.07.011

ASTM, 2017a. ASTM D7928-17, Standard Test Method for Particle-Size Distribution (Gradation) of Fine-Grained Soils Using the Sedimentation (Hydrometer) Analysis.

ASTM, 2017b. ASTM D6913 / D6913M-17, Standard Test Methods for Particle-Size

635 Distribution (Gradation) of Soils Using Sieve Analysis. doi:10.1520/D6913_D6913M-
636 17
637 ASTM, 2014a. ASTM D854 - 14, Standard Test Methods for Specific Gravity of Soil
638 Solids by Water Pycnometer. doi:10.1520/D0854-14
639 ASTM, 2014b. ASTM D2974 - 14, Standard Test Methods for Moisture, Ash, and
640 Organic Matter of Peat and Other Organic Soils. doi:10.1520/D2974-14
641 Azaroff, L., Buerger, M., 1953. The powder method in X-ray crystallography. New York.
642 McGraw-Hill Book Co.
643 Azevedo, A.A.B. de, Pressinotti, M.M.N., Massoli, M., 1981. Sedimentological studies of
644 the Botucatu and Pirambóia formations in the region of Santa Rita do Passa Quatro
645 (In portuguese). Rev. do Inst. Geológico 2, 31–38. doi:10.5935/0100-
646 929X.19810003
647 Benamghar, A., Gómez-Hernández, J.J., 2014. Factorial kriging of a geochemical
648 dataset for heavy-metal spatial-variability characterization. Environ. Earth Sci. 71,
649 3161–3170. doi:10.1007/s12665-013-2704-5
650 Benegas, L., Ilstedt, U., Roupsard, O., Jones, J., Malmer, A., 2014. Effects of trees on
651 infiltrability and preferential flow in two contrasting agroecosystems in Central
652 America. Agric. Ecosyst. Environ. 183, 185–196. doi:10.1016/j.agee.2013.10.027
653 Beven, K., Germann, P., 2013. Macropores and water flow in soils revisited. Water
654 Resour. Res. 49, 3071–3092. doi:10.1002/wrcr.20156
655 Bevington, J., Piragnolo, D., Teatini, P., Vellidis, G., Morari, F., 2016. On the spatial
656 variability of soil hydraulic properties in a Holocene coastal farmland. Geoderma
657 262, 294–305. doi:10.1016/j.geoderma.2015.08.025

658 Biswas, A., Si, B.C., 2009. Spatial relationship between soil hydraulic and soil physical
659 properties in a farm field. Can. J. Soil Sci. 89, 473–488. doi:10.4141/cjss08052
660 Bohling, G.C., Liu, G., Knobbe, S.J., Reboulet, E.C., Hyndman, D.W., Dietrich, P.,
661 Butler, J.J., 2012. Geostatistical analysis of centimeter-scale hydraulic conductivity
662 variations at the MADE site. Water Resour. Res. 48. doi:10.1029/2011WR010791
663 Botros, F.E., Harter, T., Onsoy, Y.S., Tuli, A., Hopmans, J.W., 2009. Spatial Variability of
664 Hydraulic Properties and Sediment Characteristics in a Deep Alluvial Unsaturated
665 Zone. Vadose Zo. J. 8, 276. doi:10.2136/vzj2008.0087
666 Brocca, L., Morbidelli, R., Melone, F., Moramarco, T., 2007. Soil moisture spatial
667 variability in experimental areas of central Italy. J. Hydrol. 333, 356–373.
668 doi:10.1016/j.jhydrol.2006.09.004
669 Brutsaert, W., 1967. Some methods of calculating unsaturated permeability. Trans.
670 ASAE 10, 400–404.
671 Burke, S., Mulligan, M., Thornes, J.B., 1999. Optimal irrigation efficiency for maximum
672 plant productivity and minimum water loss, in: Agricultural Water Management.
673 Elsevier, pp. 377–391. doi:10.1016/S0378-3774(99)00011-6
674 Cambardella, C.A., Moorman, T.B., Parkin, T.B., Karlen, D.L., Novak, J.M., Turco, R.F.,
675 Konopka, A.E., 1994. Field-Scale Variability of Soil Properties in Central Iowa Soils.
676 Soil Sci. Soc. Am. J. 58, 1501. doi:10.2136/sssaj1994.03615995005800050033x
677 Cassiraga, E.F., Fernàndez-Garcia, D., Gómez-Hernández, J.J., 2005. Performance
678 assessment of solute transport upscaling methods in the context of nuclear waste
679 disposal. Int. J. Rock Mech. Min. Sci. 42, 756–764.
680 doi:10.1016/j.ijrmms.2005.03.013

681 Chapuis, R.P., Dallaire, V., Marcotte, D., Chouteau, M., Acevedo, N., Gagnon, F., 2005.
682 Evaluating the hydraulic conductivity at three different scales within an unconfined
683 sand aquifer at Lachenaie, Quebec. Can. Geotech. J. 42, 1212–1220.
684 doi:10.1139/t05-045
685 Che, M., Loux, M.M., Traina, S.J., Logan, T.J., 1992. Effect of pH on Sorption and
686 Desorption of Imazaquin and Imazethapyr on Clays and Humic Acid. J. Environ.
687 Qual. 21, 698. doi:10.2134/jeq1992.00472425002100040026x
688 Corey, A.T., 1977. Mechanics of heterogeneous fluids in porous media. Mech. Heterog.
689 fluids porous media.
690 DeGroot, D.J., Baecher, G.B., 1993. Estimating Autocovariance of In-Situ Soil
691 Properties. J. Geotech. Eng. 119, 147–166. doi:10.1061/(ASCE)0733-
692 9410(1993)119:1(147)
693 Dippenaar, M.A., 2014. Porosity Reviewed: Quantitative Multi-Disciplinary
694 Understanding, Recent Advances and Applications in Vadose Zone Hydrology.
695 Geotech. Geol. Eng. 32, 1–19. doi:10.1007/s10706-013-9704-9
696 Donagema, G., Campos, D. de, 2011. Manual de métodos de análise de solo., Embrapa
697 Solos-.
698 Dyck, M.F., Kachanoski, R.G., de Jong, E., 2005. Spatial Variability of Long-Term
699 Chloride Transport under Semiarid Conditions. Vadose Zo. J. 4, 915.
700 doi:10.2136/vzj2004.0162
701 Erşahin, S., Aşkın, T., Tarakçıoğlu, C., Özenç, D.B., Korkmaz, K., Kutlu, T., Sünal, S.,
702 Bilgili, B.C., 2017. Spatial variation in the solute transport attributes of adjacent
703 Typic Haplusteps, Mollic Ustifluvents, and Lithic Ustipsamments. Geoderma 289,

107–116. doi:10.1016/j.geoderma.2016.11.035

Fagundes, J.R.T., Zuquette, L.V., 2011. Sorption behavior of the sandy residual unconsolidated materials from the sandstones of the Botucatu Formation, the main aquifer of Brazil. Environ. Earth Sci. 62, 831–845. doi:10.1007/s12665-010-0570-y

Ferreira da Silva, E., Freire Ávila, P., Salgueiro, A.R., Candeias, C., Garcia Pereira, H., 2013. Quantitative–spatial assessment of soil contamination in S. Francisco de Assis due to mining activity of the Panasqueira mine (Portugal). Environ. Sci. Pollut. Res. 20, 7534–7549. doi:10.1007/s11356-013-1495-2

Fetter, C., 1999. Contaminant hydrogeology, 2nd ed. Prentice Hall, New York.

Freeze, R., Cherry, J., 1979. Groundwater (p. 604). PrenticeHall Inc Englewood cliffs, New Jersey.

Fu, J., Gómez-Hernández, J.J., 2009. Uncertainty assessment and data worth in groundwater flow and mass transport modeling using a blocking Markov chain Monte Carlo method. J. Hydrol. 364, 328–341. doi:10.1016/j.jhydrol.2008.11.014

Giacheti, H.L., Rohm, S.A., Nogueira, J.B., Cintra, J.C.A., 1993. Geotechnical properties of the Cenozoic sediment (In protuguese), in: Albiero, J.H., Cintra, J.C.A. (Eds.), Soil from the Interior of São Paulo. ABMS, Sao Paulo, pp. 143–175.

Gómez-Hernández, J.J., Fu, J., Fernandez-Garcia, D., 2006. Upscaling retardation factors in 2-D porous media, in: Bierkens, M.F.P., Gehrels, J.C., Kovar, K. (Eds.), Calibration and Reliability in Groundwater Modelling : From Uncertainty to Decision Making : Proceedings of the ModelCARE 2005 Conference Held in The Hague, the Netherlands, 6-9 June, 2005. IAHS Publication, pp. 130–136.

Goovaerts, P., 2001. Geostatistical modelling of uncertainty in soil science. Geoderma

727 103, 3–26. doi:10.1016/S0016-7061(01)00067-2
728 Goovaerts, P., 1999. Geostatistics in soil science: State-of-the-art and perspectives.
729 Geoderma 89, 1–45. doi:10.1016/S0016-7061(98)00078-0
730 Goovaerts, P., 1998. Geostatistical tools for characterizing the spatial variability of
731 microbiological and physico-chemical soil properties. Biol. Fertil. Soils 27, 315–334.
732 doi:10.1007/s003740050439
733 Goovaerts, P., 1997. Geostatistics for natural resources evaluation. Oxford University
734 Press.
735 Goovaerts, P., 1994. Study of spatial relationships between two sets of variables using
736 multivariate geostatistics. Geoderma 62, 93–107. doi:10.1016/0016-7061(94)90030-
737 2
738 Grego, C.R., Vieira, S.R., Antonio, A.M., Della Rosa, S.C., 2006. Geostatistical analysis
739 for soil moisture content under the no tillage cropping system. Sci. Agric. 63, 341–
740 350. doi:10.1590/S0103-90162006000400005
741 Grunwald, S., Reddy, K.R., Newman, S., DeBusk, W.F., 2004. Spatial variability,
742 distribution and uncertainty assessment of soil phosphorus in a south Florida
743 wetland. Environmetrics 15, 811–825. doi:10.1002/env.668
744 Guagliardi, I., Buttafuoco, G., Cicchella, D., De Rosa, R., 2013. A multivariate approach
745 for anomaly separation of potentially toxic trace elements in urban and peri-urban
746 soils: an application in a southern Italy area. J. Soils Sediments 13, 117–128.
747 doi:10.1007/s11368-012-0583-0
748 Gupte, S., Radcliffe, D., Franklin, D., West, L., Tollner, E., Hendrix, P., 1996. Anion
749 transport in a Piedmont Ultisol: II. Local-scale parameters. Soil Sci. Soc. Am. J. 60,

762–770. doi:10.2136/sssaj1996.03615995006000030012x

Gwenzi, W., Hinz, C., Holmes, K., Phillips, I.R., Mullins, I.J., 2011. Field-scale spatial variability of saturated hydraulic conductivity on a recently constructed artificial ecosystem. Geoderma 166, 43–56. doi:10.1016/j.geoderma.2011.06.010

Hajnos, M., Lipiec, J., Świeboda, R., Sokołowska, Z., Witkowska-Walczak, B., 2006. Complete characterization of pore size distribution of tilled and orchard soil using water retention curve, mercury porosimetry, nitrogen adsorption, and water desorption methods. Geoderma 135, 307–314. doi:10.1016/j.geoderma.2006.01.010

Hillel, D., 2004. Introduction to environmental soil physics, Journal of Chemical Information and Modeling. Elsevier Academic Press. doi:10.1017/CBO9781107415324.004

Hoffmann, U., Hoffmann, T., Jurasinski, G., Glatzel, S., Kuhn, N.J., 2014. Assessing the spatial variability of soil organic carbon stocks in an alpine setting (Grindelwald, Swiss Alps). Geoderma 232–234, 270–283. doi:10.1016/j.geoderma.2014.04.038

Holland, J.M., 2004. The environmental consequences of adopting conservation tillage in Europe: Reviewing the evidence. Agric. Ecosyst. Environ. doi:10.1016/j.agee.2003.12.018

Hu, W., Shao, M.A., Wang, Q.-J., Fan, J., Reichardt, K., 2008. Spatial variability of soil hydraulic properties on a steep slope in the loess plateau of China. Sci. Agric. 65, 268–276. doi:10.1590/S0103-90162008000300007

Huang, M., Zettl, J.D., Lee Barbour, S., Pratt, D., 2016. Characterizing the spatial variability of the hydraulic conductivity of reclamation soils using air permeability.

773 Geoderma 262, 285–293. doi:10.1016/j.geoderma.2015.08.014
774 Huysmans, M., Dassargues, A., 2006. Stochastic analysis of the effect of spatial
775 variability of diffusion parameters on radionuclide transport in a low permeability
776 clay layer. Hydrogeol. J. 14, 1094–1106. doi:10.1007/s10040-006-0035-2
777 Igwe, C.A., 2005. Soil physical properties under different management systems and
778 organic matter effects on soil moisture along soil catena in southeastern Nigeria.
779 Trop. Subtrop. Agroecosystems 5.
780 Iqbal, J., Thomasson, J.A., Jenkins, J.N., Owens, P.R., Whisler, F.D., 2005. Spatial
781 Variability Analysis of Soil Physical Properties of Alluvial Soils. Soil Sci. Soc. Am. J.
782 69, 1338. doi:10.2136/sssaj2004.0154
783 Isaaks, E.H., Srivastava, R.M., 1989. An introduction to applied geostatistics. Oxford
784 University Press.
785 Jacques, D., Mouvet, C., Mohanty, B., Vereecken, H., Feyen, J., 1999. Spatial variability
786 of atrazine sorption parameters and other soil properties in a podzoluvisol. J.
787 Contam. Hydrol. 36, 31–52. doi:10.1016/S0169-7722(98)00141-7
788 Jarvis, N.J., 2007. A review of non-equilibrium water fl ow and solute transport in soil
789 macropores: Principles, controlling factors and consequences for water quality. Eur.
790 J. Soil Sci. 58, 523–546. doi:10.4141/cjss2011-050
791 Kazemi, H. V., Anderson, S.H., Goyne, K.W., Gantzer, C.J., 2008. Spatial variability of
792 bromide and atrazine transport parameters for a Udipsamment. Geoderma 144,
793 545–556. doi:10.1016/j.geoderma.2008.01.018
794 Keesstra, S.D., Geissen, V., Mosse, K., Piiranen, S., Scudiero, E., Leistra, M., van
795 Schaik, L., 2012. Soil as a filter for groundwater quality. Curr. Opin. Environ.

796 Sustain. doi:10.1016/j.cosust.2012.10.007
797 Keng, J.C., Uehara, G., 1974. Chemistry, mineralogy, and taxonomy of oxisols and
798 ultisols. Proc. Soil Crop Sci. Soc. Florida 33, 119–926.
799 Koorevaar, P., Menelik, G., Dirksen, C., 1983. Elements of Soil Physics, 1st ed,
800 Developments in Soil Science (p.1-36). Elsevier Science, Amsterdam.
801 doi:10.1016/S0166-2481(08)70048-5
802 Kronberg, B.I., Fyfe, W.S., Leonardos, O.H., Santos, A.M., 1979. The chemistry of some
803 Brazilian soils: Element mobility during intense weathering. Chem. Geol. 24, 211–
804 229. doi:10.1016/0009-2541(79)90124-4
805 Kung, K.-J.S., Hanke, M., Helling, C.S., Kladivko, E.J., Gish, T.J., Steenhuis, T.S.,
806 Jaynes, D.B., 2005. Quantifying Pore-Size Spectrum of Macropore-Type
807 Preferential Pathways. Soil Sci. Soc. Am. J. 69, 1196. doi:10.2136/sssaj2004.0208
808 Lacasse, S., Nadim, F., 1996. Uncertainties in characterising soil properties. Publ. -
809 Norges Geotek. Inst. 201, 49–75.
810 Lapidus, L., Amundson, N., 1952. Mathematics of adsorption in beds VI. The effect of
811 longitudinal diffusion in ion exchange and chromatographic columns. J. Phys.
812 Chem. 984–988. doi:10.1021/j150500a014
813 Li, L., Zhou, H., Gómez-Hernández, J.J., 2011. Transport upscaling using multi-rate
814 mass transfer in three-dimensional highly heterogeneous porous media. Adv. Water
815 Resour. 34, 478–489. doi:10.1016/j.advwatres.2011.01.001
816 Lipiec, J., Walczak, R., Witkowska-Walczak, B., Nosalewicz, A., Słowińska-Jurkiewicz,
817 A., Sławiński, C., 2007. The effect of aggregate size on water retention and pore
818 structure of two silt loam soils of different genesis. Soil Tillage Res. 97, 239–246.

doi:10.1016/j.still.2007.10.001

Liu, L., Cheng, Y.-M., Jiang, S.-H., Zhang, S.-H., Wang, X.-M., Wu, Z.-H., 2017. Effects of spatial autocorrelation structure of permeability on seepage through an embankment on a soil foundation. Comput. Geotech. 87, 62–75. doi:10.1016/j.compgeo.2017.02.007

Mahapatra, I.C., Singh, K.N., Pillai, K.G., Bapat, S.R., 1985. Rice soils and their management. Indian J. Agron. 1–41.

Marín-Castro, B.E., Geissert, D., Negrete-Yankelevich, S., Gómez-Tagle Chávez, A., 2016. Spatial distribution of hydraulic conductivity in soils of secondary tropical montane cloud forests and shade coffee agroecosystems. Geoderma 283, 57–67. doi:10.1016/j.geoderma.2016.08.002

Massey, F.J., 1951. The Kolmogorov-Smirnov Test for Goodness of Fit. J. Am. Stat. Assoc. 46, 68–78. doi:10.1080/01621459.1951.10500769

Mbagwu, J.S.C., 1995. Saturated hydraulic conductivity in relation to physical properties of soils in the Nsukka Plains, southeastern Nigeria. Geoderma 68, 51–66. doi:10.1016/0016-7061(95)00024-I

Mekaru, T., Uehara, G., 1972. Anion adsorption in ferruginous tropical soils. Soil Sci. Soc. Am. doi:10.2136/sssaj1972.03615995003600020027x

Miranda, M.J. de, Pinto, H.S., Júnior, J.Z., Fagundes, R.M., Fonsechi, D.B., Calve, L., Pelllegrino, G.Q., 2015. Climate of the Paulista municipalities (In portuguese) [WWW Document]. CEPAGRI (Centro Pesqui. Meteorológicas e Climáticas Apl. à Agric.

Motaghian, H.R., Mohammadi, J., 2011. Spatial estimation of saturated hydraulic

conductivity from terrain attributes using regression, kriging, and artificial neural networks. Pedosphere 21, 170–177. doi:10.1016/S1002-0160(11)60115-X

Mulla, D., Mc Bratney, A., 2002. Soil spatial variability, in: Warrick, A. (Ed.), Soil Physics Companion. CRC Press, Boca Raton, pp. 343–373. doi:10.2136/vzj2004.0727

Nanzyo, M., Shoji, S., Dahlgren, R., 1993. Volcanic Ash Soils - Genesis, Properties and Utilization. Dev. Soil Sci. 21, 189–207. doi:10.1016/S0166-2481(08)70268-X

Narwal, R.P., 2002. Unique properties of volcanic ash soils. Glob. J. Environ. Res. 6, 99–112.

Nemes, A., Timlin, D.J., Pachepsky, Y.A., Rawls, W.J., 2009. Evaluation of the Pedotransfer Functions for their Applicability at the U.S. National Scale. Soil Sci. Soc. Am. J. 73, 1638. doi:10.2136/sssaj2008.0298

Ogata, A., Banks, R.B., 1961. A solution of the differential equation of longitudinal dispersion in porous media, US Geological Survey Professional Papers. doi:10.3133/pp411A

Pachepsky, Y., Rawls, W.J., 2004. Development of Pedotransfer Functions in Soil Hydrology. Elsevier Science.

Papanicolaou, A. (Thanos) N., Elhakeem, M., Wilson, C.G., Lee Burras, C., West, L.T., Lin, H. (Henry), Clark, B., Oneal, B.E., 2015. Spatial variability of saturated hydraulic conductivity at the hillslope scale: Understanding the role of land management and erosional effect. Geoderma 243–244, 58–68. doi:10.1016/j.geoderma.2014.12.010

Peel, M.C., Finlayson, B.L., McMahon, T.A., 2007. Updated world map of the Köppen-Geiger climate classification. Hydrol. Earth Syst. Sci. 11, 1633–1644. doi:10.5194/hess-11-1633-2007

865 Pejon, O., 1992. Mapeamento geotécnico regional da folha de Piracicaba (SP): Estudos
866 de aspectos metodológicos de caracterização e apresentação de atributos.
867 Universidade de São Paulo, Tese de doutorado (in Portuguese). University of São
868 Paulo.
869 Porfiri, C., Montoya, J.C., Koskinen, W.C., Azcarate, M.P., 2015. Adsorption and
870 transport of imazapyr through intact soil columns taken from two soils under two
871 tillage systems. Geoderma 251–252, 1–9. doi:10.1016/j.geoderma.2015.03.016
872 Rodríguez Martín, J.A., Vázquez de la Cueva, A., Grau Corbí, J.M., López Arias, M.,
873 2007. Factors Controlling the Spatial Variability of Copper in Topsoils of the
874 Northeastern Region of the Iberian Peninsula, Spain. Water. Air. Soil Pollut. 186,
875 311–321. doi:10.1007/s11270-007-9487-9
876 Rohm, S.A., 1992. Shear strength of a non-saturated lateritic sandy soil in the São
877 Carlos region (In portuguese). University of Sao Paulo.
878 Salamon, P., Fernàndez-Garcia, D., Gómez-Hernández, J.J., 2007. Modeling tracer
879 transport at the MADE site: The importance of heterogeneity. Water Resour. Res.
880 43. doi:10.1029/2006WR005522
881 Santos, H.G. dos, Jacomine, P.K.T., Anjos, L.H.C. dos, Oliveira, V.Á. de, Lumbreras,
882 J.F., Coelho, M.R., Almeida, J.A. de, Cunha, T.J.F., Oliveira, J.B. de, 2014.
883 Brazilian system of soil classification (In portuguese), 4th ed. EMBRAPA. Centro
884 Nacional de Pesquisa de Solos, Brasília, DF.
885 Silva, L.P. da, van Lier, Q. de J., Correa, M.M., Miranda, J.H. de, Oliveira, L.A. de, 2016.
886 Retention and Solute Transport Properties in Disturbed and Undisturbed Soil
887 Samples. Rev. Bras. Ciência do Solo 40. doi:10.1590/18069657rbcs20151045

888 Sobieraj, J.A., Elsenbeer, H., Coelho, R.M., Newton, B., 2002. Spatial variability of soil
889 hydraulic conductivity along a tropical rainforest catena. Geoderma 108, 79–90.
890 doi:10.1016/S0016-7061(02)00122-2
891 Soil Survey Staff, 1999. Soil Taxonomy: A Basic System of Soil Classification for Making
892 and Interpreting Soil Surveys, Agriculture Handbook Number 436. Blackwell
893 Publishing Ltd, Washington, D.C. doi:10.1111/j.1475-2743.2001.tb00008.x
894 Søvik, A.K., Aagaard, P., 2003. Spatial variability of a solid porous framework with
895 regard to chemical and physical properties. Geoderma 113, 47–76.
896 doi:10.1016/S0016-7061(02)00315-4
897 Sudicky, E.A., Illman, W.A., Goltz, I.K., Adams, J.J., McLaren, R.G., 2010. Heterogeneity
898 in hydraulic conductivity and its role on the macroscale transport of a solute plume:
899 From measurements to a practical application of stochastic flow and transport
900 theory. Water Resour. Res. 46. doi:10.1029/2008WR007558
901 Teixeira, D.D.B., Bicalho, E. da S., Panosso, A.R., Perillo, L.I., Iamaguti, J.L., Pereira,
902 G.T., La Scala Jr, N., 2012. Uncertainties in the prediction of spatial variability of soil
903 CO2 emissions and related properties. Rev. Bras. Ciência do Solo 36, 1466–1475.
904 doi:10.1590/S0100-06832012000500010
905 Tesfahunegn, G.B., Tamene, L., Vlek, P.L.G., 2011. Catchment-scale spatial variability
906 of soil properties and implications on site-specific soil management in northern
907 Ethiopia. Soil Tillage Res. 117, 124–139. doi:10.1016/j.still.2011.09.005
908 Trangmar, B.B., Yost, R.S., Uehara, G., 1986. Application of Geostatistics to Spatial
909 Studies of Soil Properties. Adv. Agron. 38, 45–94. doi:10.1016/S0065-
910 2113(08)60673-2

van Genuchten, M.T., 1980. Determining transport parameters from solute displacement experiments.

van Genuchten, M.T., Wierenga, P.J., 1976. Mass Transfer Studies in Sorbing Porous Media I. Analytical Solutions1. Soil Sci. Soc. Am. J. 40, 473. doi:10.2136/sssaj1976.03615995004000040011x

Vanderborght, J., Vereecken, H., 2007. Review of Dispersivities for Transport Modeling in Soils. Vadose Zo. J. 6, 29. doi:10.2136/vzj2006.0096

Vieira, S.R., 1997. Variabilidade Espacial De Argila, Silte e Atributos Químicos Em Uma Parcela Experimental De Um Latossolo Roxo De Campinas. Bragantia 56, 181–190. doi:10.1590/S0006-87051997000100019

Wackernagel, H., 1995. Multivariate geostatistics: an introduction with applications. Multivar. geostatistics an Introd. with Appl. 387. doi:10.1016/S0098-3004(97)87526-7

Wang, Y., Zhang, X., Huang, C., 2009. Spatial variability of soil total nitrogen and soil total phosphorus under different land uses in a small watershed on the Loess Plateau, China. Geoderma 150, 141–149. doi:10.1016/j.geoderma.2009.01.021

Wang, Y.Q., Shao, M.A., 2013. Spatial Variability Of Soil Physical Properties In A Region Of The Loess Plateau Of Pr China Subject To Wind And Water Erosion. L. Degrad. Dev. 24, 296–304. doi:10.1002/ldr.1128

Washburn, E.W., 1921. Note on a method of determining the distribution of pore sizes in a porous material. Proc. Natl. Acad. Sci. U. S. A. 7, 115–116. doi:10.1073/pnas.7.4.115

Webster, R., 2001. Statistics to support soil research and their presentation. Eur. J. Soil

Sci. 52, 331–340. doi:10.1046/j.1365-2389.2001.00383.x

Wilding, L.P., Drees, L.R., 1983. Spatial variability and pedology, in: Wilding, L.P., Smeck, N.E., Hall, G.F. (Eds.), Pedogenesis and Soil Taxonomy : The Soil Orders. Elsevier, Netherlands, pp. 83–116.

Zhao, Y., Peth, S., Hallett, P., Wang, X., Giese, M., Gao, Y., Horn, R., 2011. Factors controlling the spatial patterns of soil moisture in a grazed semi-arid steppe investigated by multivariate geostatistics. Ecohydrology 4, 36–48. doi:10.1002/eco.121

Zimmermann, B., Elsenbeer, H., 2008. Spatial and temporal variability of soil saturated hydraulic conductivity in gradients of disturbance. J. Hydrol. 361, 78–95. doi:10.1016/j.jhydrol.2008.07.027

Zuquette, L.V., Palma, J.B., 2006. Avaliação da condutividade hidráulica em área de recarga do aqüífero Botucatu. Rem Rev. Esc. Minas 59, 81–87. doi:10.1590/S0370-44672006000100011

950 **List of Figures**

951

952 **Fig. 1 Location of the study site and the position of the sampling points**

953

954 **Fig. 2 Column experiments in progress: a) water deionizers, b) hydraulic head**
955 **controller device, c) rigid-wall permeameters**

956

957 **Fig. 3 Variation of the correlation coefficient among variables with the spatial**
958 **scale**

959

960 **Figure 1**

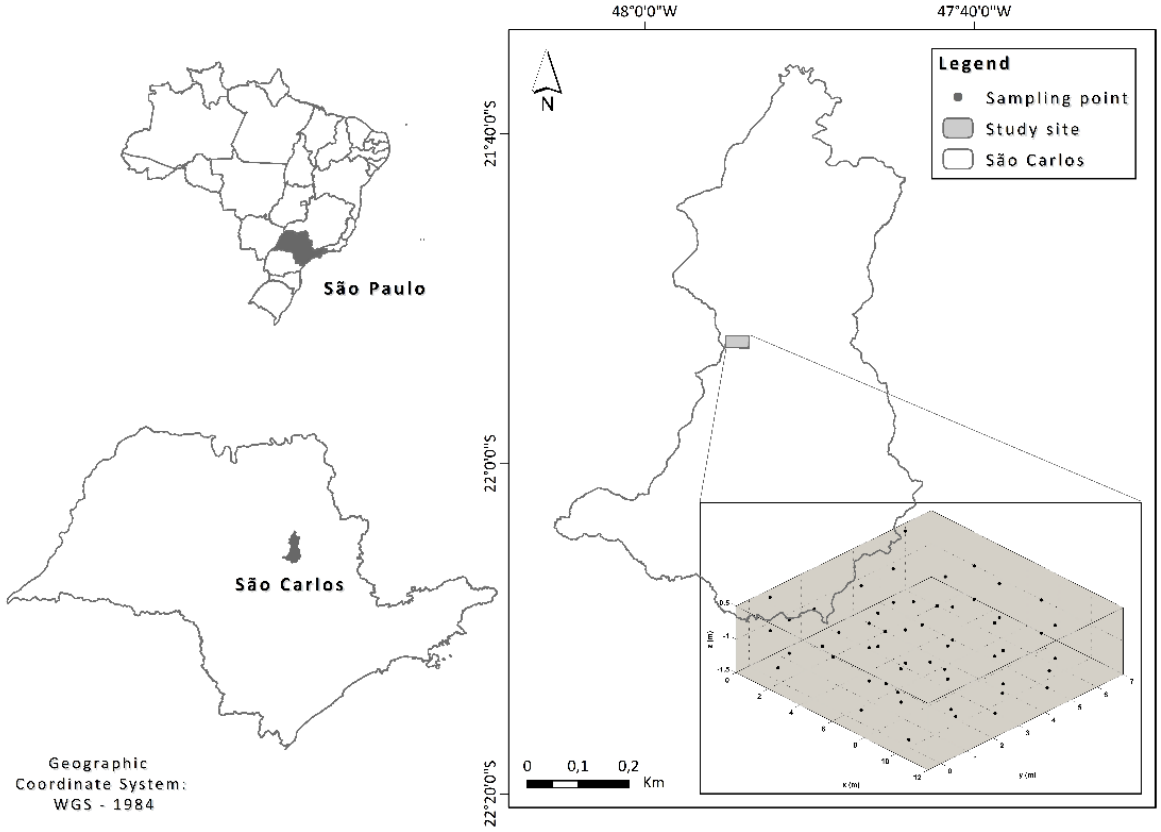

961

962

963 **Figure 2**

964

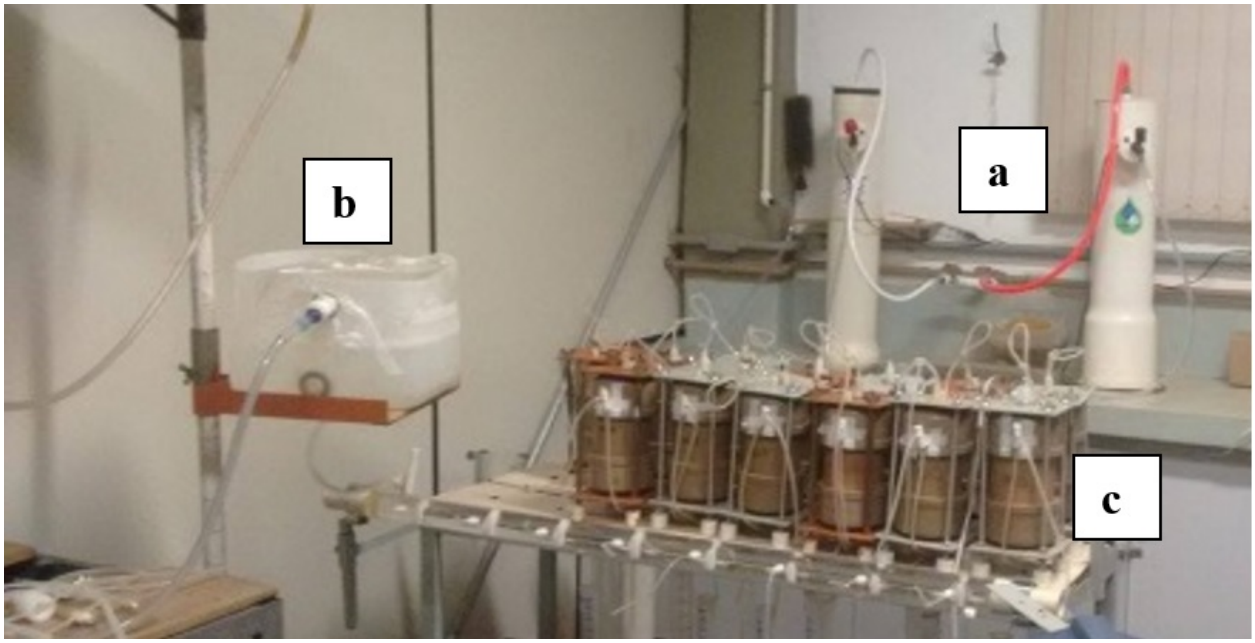

965

966

967 **Figure 3**

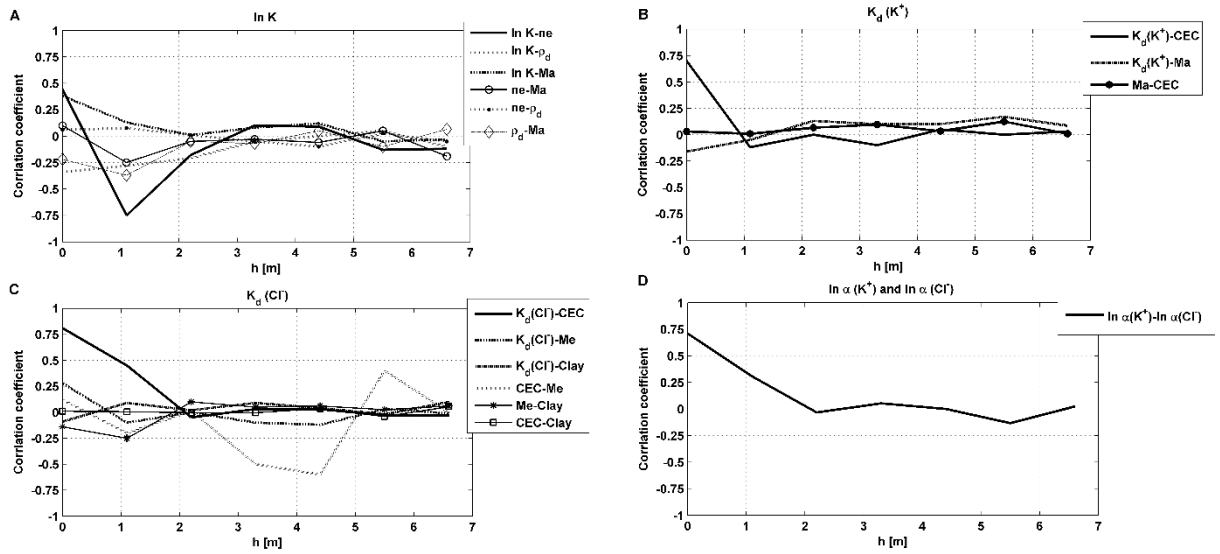

968

969

970 **List of Tables**

971

Table 1

	Mean	SD	CV	Skew	Kurt	Min	Max
K [m d^{-1}]	1.35	1.65	1.22	2.39	5.84	0.03	7.46
v [m d^{-1}]	5.40	6.57	1.23	2.20	4.61	0.13	27.71
$ln\ K$ [ln (m d^{-1})]	-0.37	1.25	n.d	-0.29	-0.12	-3.68	2.03
n [ ]	0.51	0.04	0.08	-0.24	-0.39	0.42	0.58
ne [ ]	0.24	0.02	0.08	-0.39	-0.14	0.20	0.28
ρ_d [g cm^{-3}]	1.34	0.10	0.07	0.28	-0.32	1.14	1.59
CEC [$cmol_c$ Kg^{-1}]	2.51	0.64	0.25	1.06	0.39	1.60	4.20
sand (%)	56.20	3.24	0.06	-0.36	-0.52	48.50	61.50
silt (%)	4.62	2.82	0.61	0.16	-0.06	1.40	11.40
clay (%)	39.18	3.51	0.09	0.10	-0.87	32.50	46.10
Ma [ ]	0.072	0.04	0.56	0.75	-0.58	0.031	0.152
Mi [ ]	0.262	0.06	0.23	-0.25	-0.96	0.141	0.361
Me [ ]	0.172	0.05	0.29	0.21	-0.92	0.091	0.263

SD: standard deviation, CV: coefficient of variation, Skew: Skewness, Kurt: Kurtosis, Min: minimum value, Max: maximum value, n.d: undetermined, K: hydraulic conductivity; v: linear average velocity, ρ_d: bulk density, n: total porosity, ne: effective porosity Ma: macroporosity, Me: mesoporosity, Mi: microporosity, CEC: cation exchange capacity.

992 Table 2
993

	Mean	SD	CV	Skew	Kurt	Min	Max
P (K^+) [ ]	2.07	2.12	1.02	2.15	5.61	0.11	10.80
R (K^+) [ ]	5.37	5.10	0.95	4.51	25.31	0.69	36.19
Kd (K^+) [cm^3g^{-1}]	1.71	2.27	1.33	5.61	36.75	0.01	16.75
D (K^+) [m^2d^{-1}]	1.07	1.77	1.65	2.64	7.42	0.02	8.77
α (K^+) [m]	0.18	0.19	1.06	1.82	3.32	0.01	0.88
ln α (K^+) [ln (m)]	-2.21	1.11	n.d	-0.45	0.71	-5.79	-0.12
P (Cl^-) [ ]	2.82	2.78	0.99	2.08	4.25	0.44	13.41
R (Cl^-) [ ]	2.35	1.29	0.55	0.61	-0.60	0.33	5.20
Kd (Cl^-) [cm^3g_{-1}]	0.55	0.51	0.93	0.66	-0.81	0.03	1.64
D (Cl^-) [m^2d^{-1}]	0.61	1.14	1.87	3.43	12.26	0.01	5.62
α (Cl^-) [m]	0.10	0.08	0.80	1.23	1.43	0.01	0.34
ln α (Cl^-) [ln (m)]	-2.61	0.93	n.d	-1.18	2.80	-6.18	-1.07

994 SD: standard deviation, CV: coefficient of variation, Skew: Skewness, Kurt: Kurtosis,
995 Min: minimum value, Max: maximum value, n.d.: undetermined, *P*: Peclet number, *R*:
996 retardation coefficient, K_d: partition coefficient, *D*: hydrodynamic dispersion coefficient, *α*:
997 dispersivity, (K^+) potassium, (Cl^-): chloride.
998

999 **Table 3**

	ln α (Cl^-)	*ln α* (K^+)	K_d (K^+)	K_d (Cl^-)	*CEC*	*lnK*	ρ_d	*n*	*ne*	sand	silt	clay	*Mi*	*Me*	*Ma*
ln α (Cl^-)	1.00														
ln α (K^+)	0.71**	1.00													
K_d (K^+)	-0.03	0.06	1.00												
K_d (Cl^-)	-0.09	0.10	0.63**	1.00											
CEC	-0.04	0.15	0.70**	0.81**	1.00										
ln K	0.13	0.11	-0.02	-0.14	-0.10	1.00									
ρ_d	0.33*	0.11	-0.22	-0.20	-0.26	-0.34*	1.00								
n	-0.32*	-0.10	0.23	0.19	0.26	0.33*	-0.99**	1.00							
ne	0.25	0.12	0.06	0.02	-0.01	0.44**	0.06	-0.06	1.00						
sand	0.21	0.18	-0.27	-0.13	-0.17	0.01	0.22	-0.22	-0.28	1.00					
silt	-0.07	-0.10	0.16	0.30*	0.21	0.05	-0.10	0.08	0.11	-0.29*	1.00				
clay	-0.14	-0.10	0.15	-0.09	0.01	-0.05	-0.11	0.13	0.16	-0.69**	-0.48**	1.00			
Mi	-0.21	-0.18	-0.39**	-0.25	-0.26	-0.02	0.04	-0.03	-0.22	0.10	-0.37**	0.18	1.00		
Me	0.08	0.06	0.36*	0.28	0.12	-0.19	0.18	-0.20	0.22	-0.15	0.40**	-0.14	-0.68**	1.00	
Ma	0.10	0.03	-0.16	-0.20	0.03	0.38**	-0.22	0.24	0.10	0.14	-0.02	-0.12	0.28	-0.63**	1.00

1000

1001 *α*: dispersivity, (K^+) potassium, (Cl^-): chloride, K_d: partition coefficient, *CEC*: cation exchange capacity, *K*:
1002 hydraulic conductivity; ρ_d: bulk density, *n*: total porosity, *ne*: effective porosity, *Mi:* microporosity, *Me*:
1003 mesoporosity, *Ma*: macroporosity
1004 * significant at 0.01 level of significance.
1005 ** significant at 0.05 level of significance.
1006

Table 4

	K_d (K^+)	*ln α* (K^+)	K_d (Cl^-)	*ln α* (Cl^-)	*ln K*
ln K	-	-	-	-	
n	-	-	-	-	-
ne	-	-	-	-	26.4
ρ_d	-	-	-	-	-3.90
CEC	0.68	-	0.48	-	-
sand	-	-	-	-	-
silt	-	-	-	-	-
clay	-	-	0.03	-	-
Ma	-0.03	-	-	-	0.09
Mi	-	-	-	-	-
Me	-	-	0.02	-	-
K_d (K^+)		-	-	-	-
ln α (K^+)	-		-	0.63	-
K_d (Cl^-)	-	-		-	-
ln α (Cl^-)	-	0.79	-		-
Intercept	-0.29	-0.26	-2.34	-1.15	-2.25
R^2	0.70	0.50	0.60	0.50	0.40
r*	0.84	0.70	0.77	0.72	0.63

* Pearson's coefficient

All results were significant at p =< 0.05

1015 **Table 5**

1016

Variable	Model	Nugget (c_0)	Sill (c_1)	Range (m) (a)
ln K	Spherical	0.0	1.0	4.0
n	Spherical	0.0	1.0	3.0
ne	Spherical	0.0	1.0	3.0
ρ_d	Spherical	0.0	1.0	3.5
CEC	Spherical	0.0	1.0	3.0
sand	Spherical	0.0	1.0	3.0
silt	Spherical	0.0	1.0	2.5
clay	Pure nugget effect	1.0	0.0	-
Ma	Spherical	0.0	1.0	3.5
Mi	Spherical	0.45	0.55	2.5
Me	Spherical	0.00	1.0	3.0
K_d (K^+)	Spherical	0.40	0.60	3.6
ln α (K^+)	Spherical	0.50	0.50	3.0
K_d (Cl^-)	Spherical	0.55	0.45	3.3
ln α (Cl^-)	Spherical	0.30	0.70	2.7

1017

1018

1019

1020

1021